

## Interplume as source of the fast solar wind

L. Teriaca<sup>1</sup> \*, G. Poletto<sup>1</sup>, M. Romoli<sup>2</sup> and D. A. Biesecker<sup>3</sup>

<sup>1</sup> INAF/Osservatorio Astrofisico di Arcetri, 50125 Firenze, Italy  
e-mail: lte@arcetri.astro.it

<sup>2</sup> Dipartimento di Astronomia e Scienza dello Spazio, Università di Firenze,  
50125 Firenze, Italy

<sup>3</sup> NOAA/Space Environment Center, 325 Broadway, Boulder, CO 80305, USA

**Abstract.** High speed solar wind is known to originate in polar coronal holes which, however, are made up of two components: bright, high density regions known as *plumes* and dark, weakly emitting low density regions known as *interplumes*. Recent space observations have shown that the width of UV lines is larger in interplume regions. Moreover, observations of the ratio of the O VI doublet lines at 1032 and 1037 Å, at 1.7  $R_{\odot}$ , suggest higher outflows in interplume regions than in plumes at that altitude. In this work we examine SUMER and UVCS observations of a north polar coronal hole taken on 1996 June 3, over the altitude range between 1 and 2  $R_{\odot}$  and, through a Doppler dimming analysis of our data, we show that interplume areas may be really identified as sources of fast wind streams. The behavior of plumes, on the contrary, can be interpreted in terms of static structures embedded in the interplume ambient. We conclude comparing our results with the predictions of theoretical models of the solar wind.

**Key words.** Solar Physics – Coronal holes – Wind acceleration

### 1. Introduction

Polar coronal holes have long been recognized to be the sources of the high speed solar wind (Krieger et al. 1973), but not much is known, yet, about where, within coronal holes, the solar wind originates. White light, UV and soft X-rays images of polar coronal holes reveal denser features

– rays and plumes – showing up within the low density interplume plasma and preserving their identity out to large distances (see e.g. DeForest et al. 2001).

Analyses of SUMER (e.g. Banerjee et al. 2000) and UVCS (e.g. Giordano et al. 2000) data have shown that the width of UV lines in interplumes is larger than in plume regions, hinting to interplumes as the site where energy is preferentially deposited and, possibly, fast wind emanates. Moreover, Giordano et al. (2000), from a Doppler dimming analysis of the O VI 1032 and 1037 Å lines at 1.7  $R_{\odot}$ , found

---

*Send offprint requests to:* L. Teriaca

\* now at Max Planck Institut für Aeronomie,  
D-37191 Katlenburg-Lindau, Germany

*Correspondence to:* Osservatorio Astrofisico di  
Arcetri, Largo Enrico Fermi 5, 50125 Firenze

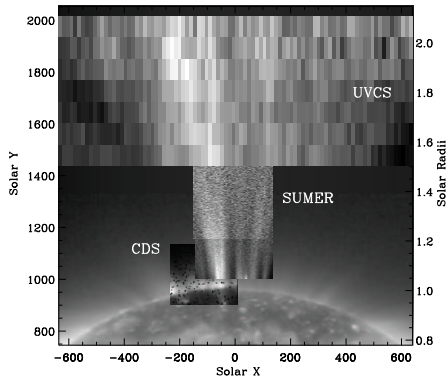


**Fig. 1.** Composite map of the 1996 June 3 north polar coronal hole as obtained using four of the instruments aboard SoHO. Bright plumes and dark interplume lanes can be identified in this diagram out to  $2.0 R_{\odot}$  above the limb. In particular, a SUMER scan in the O VI 1032 Å line shows the plume evolution with altitude up to  $1.5 R_{\odot}$ . Above this altitude the structure of the coronal hole is obtained throughout seven spectra acquired in the O VI 1032 Å line with the UVCS slit normal to the solar radius. The contrast of the SUMER and UVCS maps was enhanced by dividing each map for its average intensity profile in the  $y$ -direction.

a larger outflow speed in interplume than in plumes. Although these analyses seem to support interplumes as sources of fast wind, they refer to different holes, observed at different times and report on outflow values at only one level in the corona, rather than providing the outflow speed profile needed to understand the process of wind acceleration in the low corona.

In this paper we present the interplume outflow speed *vs.* height profile between 1 and  $2 R_{\odot}$  derived from the Doppler dimming analysis of our data and we show how plume observations can, instead, be interpreted on the basis of a static plasma. A comparison with a theoretical solar wind model concludes the paper.

## 2. Observations and Results

The observations discussed here were acquired using several instruments aboard SoHO on 1996 June 3 and are shown and described in Fig. 1. After selecting a plume and an interplume region, binning was applied to SUMER and UVCS data to increase adequately the S:N ratio. In such a way, line profiles were determined at 19 different locations above the solar limb for both plume and interplume areas. In the solar corona, the O VI 1032 and 1037 Å and the H I Ly  $\alpha$  lines are formed by electron impact excitation (collisional component) and by resonant scattering (radiative component) of the radiation coming from the disk (see e.g. Noci et al. 1987). Very schematically,

$$I_{obs} = 0.83 \frac{\Delta E}{4\pi} A_{el} \times [S_{Rad.} + S_{Coll.}]$$

where

$$\begin{aligned} S_{Rad} &= B \langle D(T_{Ion}, V_{out}, I_{\odot}) R(T_e) N_e \rangle \\ S_{Coll} &= \langle q(T_e) R(T_e) N_e^2 \rangle \end{aligned} \quad (1)$$

where  $\Delta E$  is the energy of the transition,  $A_{el}$  is the element abundance relative to hydrogen,  $q(T_e)$  the collisional excitation rate coefficient,  $N_e$  the electron number density,  $B$  the Einstein absorption coefficient,  $R(T_e)$  is the ionic fraction calculated in ionization equilibrium, and 0.83 is the value of the hydrogen to electron number density ratio for a fully ionized plasma with 10% of helium.  $D(T_{Ion}, V_{out}, I_{\odot})$  accounts for Doppler dimming and geometrical dilution factors and is function of the ion temperature  $T_{Ion}$  (consisting of the parallel  $T_{Ion}^{\parallel}$  and perpendicular  $T_{Ion}^{\perp}$  components to the direction of the magnetic field lines), the wind velocity  $V_{out}$  and the disk-averaged line intensity  $I_{\odot}$ . The quantities in brackets  $\langle \dots \rangle$  are integrated along the line of sight. In these conditions the intensity of the resonantly scattered component of a coronal line is a function of the speed component along the magnetic field lines ( $V_{out}$ ). This means that, knowing the atomic parameters of the transition, the physical characteristics of the emitting plasma (such as

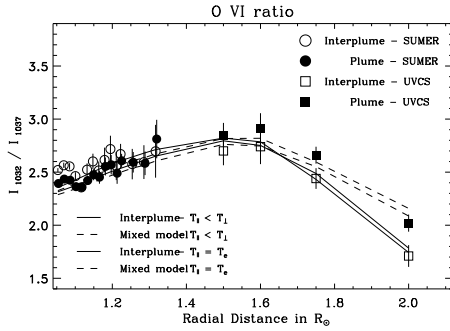


**Fig. 2.** O VI 1032 to O VI 1037 intensity line ratio as a function of altitude in polar coronal holes. Solid lines represent models for interplume conditions in the anisotropic (thin lines) and partially isotropic case (thick lines). Dashed lines represent a mixed model comprising plume and interplume lanes.

its chemical composition, electron density, electron temperature,  $T_{Ion}^{\parallel}$  and  $T_{Ion}^{\perp}$  and the disk radiance, we are able to determine the outflow speed profile that reproduces our observations. Many of these parameters can be constrained by our observations and/or through values given in the literature, while others are free parameters which we vary in order to explore the dependence of the outflow speed on the physical properties of the emitting region. Because our observations were acquired at the north pole, we can assume the magnetic field lines to be perpendicular to the line of sight. This allows us to identify  $T_o^{\perp}$  with the effective temperature  $T_{eff}$  associated with the Doppler width (in  $\text{km s}^{-1}$ ) of the observed spectral line.

Both cases of  $T_o^{\parallel}$  equal to  $T_e$  (anisotropic case) and  $T_o^{\parallel}$  equal to  $T_o^{\perp}$  (isotropic case) have been explored. For this work we adopted the  $T_e$  values given by Wilhelm et al. (1998) below  $1.2 R_{\odot}$  and we assumed constant temperature above this altitude.

Above  $1.5 R_{\odot}$  average electron densities were obtained from the UVCS WLC and the LASCO C2 coronagraph for the

day of our observations. The behaviour at lower altitudes was evaluated from data published by Wilhelm et al. (1998) for both plume and interplume regions. The integrated disk radiance of the O VI 1032 was evaluated assuming a  $1/\cos(\theta)$  center-to-limb line intensity variation (Wilhelm et al. 1998b) and adopting a radiance at disk centre of  $300 \text{ erg cm}^{-2} \text{ s}^{-1} \text{ st}^{-1}$ . For the H I Ly  $\alpha$  the disk radiance was obtained from SOLSTICE data.

Using those electron density and temperature profiles the O VI 1032 and 1037 observed line intensity ratios below  $1.2 R_{\odot}$  were reproduced by means of Eqs. 1 assuming no outflow speed. In these conditions ( $V_{out} = 0$ ), O VI line intensities depend on the elemental abundance only (once the density and temperature profiles have been fixed). We found that observed line intensities below  $1.2 R_{\odot}$  could be reproduced adopting an oxygen abundance of 8.5.

Using the adopted interplume  $T_e$  and  $N_e$  profiles and an oxygen abundance of 8.5, we found the outflow profile that reproduces the observed interplume O VI line ratios (see Fig. 2) as well as the observed O VI and H I Ly  $\alpha$  line radiances for isotropic and anisotropic conditions. Fig. 3 shows the obtained interplume outflow speed profiles for both O VI and H I ions.

A realistic attempt to model our plumes observations requires a combination of plume and interplume emissivities along the line of sight. A mixed plume-interplume model has been created assuming a single plume with no outflowing plasma embedded in the outflowing interplume plasma. The line of sight fraction occupied by the plume was estimated from Fig. 1. This model is able to reproduce our plume observations (see Fig. 2) supporting the hypothesis that interplumes are the regions where fast wind streams originate.

### 3. Discussion and Conclusions

The results presented here provide strong evidence in favor of interplume regions as sources of fast wind streams: we have shown

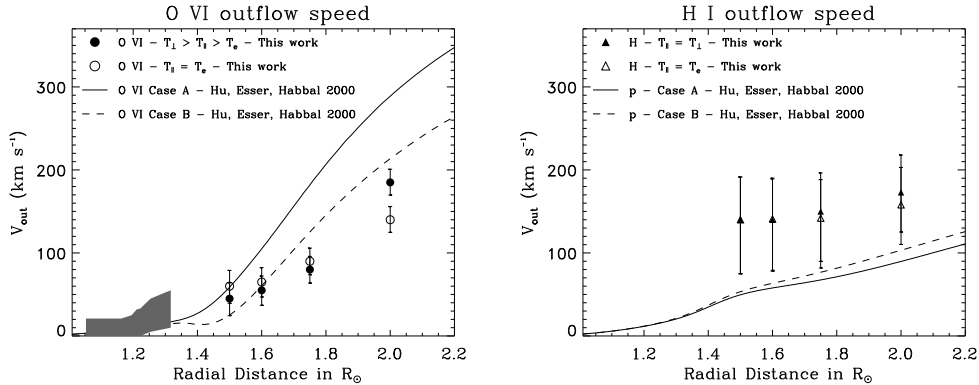


**Fig. 3.** O VI ions (left panel) and H I atoms (right panel) outflow speed in interplume lanes between 1 and 2  $R_{\odot}$ . Filled symbols refers to the isotropic models, while open symbols indicate the results for the anisotropic model. The shaded area between 1.05 and 1.3  $R_{\odot}$  indicates speed values compatible with SUMER data. Outflow speed profiles, obtained by Hu et al. (2000) for O VI ions and protons including (Case A) and ignoring (Case B) the dispersive effect of minor ions, are shown using solid and dashed lines, respectively.

that the physical parameters of the interplume ambient are compatible with the presence of an outflowing plasma, while plume observations can be explained on the basis of a static plume, embedded in interplume regions. We also provide, for the first time, a profile of the plasma outflow speed vs. height, between 1 and 2 solar radii, for O VI ions.

Our results can be also compared with the outflow speed obtained by Hu et al. (2000) in a four-fluid solar wind model based on the dissipation of high frequency ion cyclotron waves. These authors made the calculation, for both O VI ions and protons, including (Case A) and ignoring (Case B) the dispersive effect of minor ions. Fig. 3 shows (left panel) the O VI outflow profiles obtained for both semi-isotropic (filled circles) and anisotropic conditions (open circles) together with the outflow speeds calculated by Hu et al. (2000).

Similarly, the right panel compares the results for H I ions with those obtained by Hu et al. (2000) for protons. In the left panel, the good agreement between the model and

the observations is clear, and shows that predictions from the theory of heavy ion acceleration by ion-cyclotron waves are consistent with observational results. However, further work is probably required to explain H/proton acceleration, which is possibly confined to lower altitudes than those where oxygen ions are being accelerated and may have a steeper speed profile than suggested by theoretical models.

*Acknowledgements.* The work of L.T. has been supported by ASI and MIUR. SOHO is a mission of international cooperation between ESA and NASA.

## References

- Banerjee, D. et al. 2000, Sol. Phys. 194, 43
- DeForest, C. E. et al. 2001, ApJ 546, 569
- Giordano, S. et al. 2000, ApJ 531, L79
- Hu, Y.Q. et al. 2000, JGR 105, 5093
- Krieger, A. S. et al. 1973, Sol. Phys. 29, 505
- Noci, G. et al. 1987, ApJ 315, 706
- Wilhelm, K. et al. 1998, ApJ 500, 1023
- Wilhelm, K. et al. 1998b, A&A 334, 685